JOURNAL OF CATALYSIS **161,** 78–86 (1996)
ARTICLE NO. 0164

Characteristic Features of Raman Band Shifts of Scheelite-Type Molybdate Catalysts Exchanged with the ^{18}O Tracer via Redox Reactions

Takehiko Ono,[1] Nobuaki Ogata, and Yasuhiro Miyaryo

Department of Applied Chemistry, University of Osaka Prefecture, 1-1 Gakuencho, Sakai, Osaka 593, Japan

Received September 30, 1994; revised December 11, 1995; accepted January 29, 1996

The oxide oxygen of scheelite-type α-$MnMoO_4$, β-$CoMoO_4$, and α-$Bi_2Mo_3O_{12}$ were exchanged with the ^{18}O tracer using a reduction–oxidation method. The Raman band shifts in the spectra of these catalysts were examined. Normal coordination analysis and diatomic approximation reported in previous literature have shown that the Raman bands are correlated to the Mo–O stretchings of these molybdate catalysts. With α-$MnMoO_4$, the band at 945 cm^{-1} corresponding to the shortest Mo=O of a Mo tetrahedron was exchanged preferentially while with β-$CoMoO_4$, which is isotypic with α-$MnMoO_4$, all the oxygen of Mo tetrahedra were exchanged with an increase in the ^{18}O exchange. With α-$Bi_2Mo_3O_{12}$ which has two twin Mo tetrahedra, the bands at 865 and 845 cm^{-1} were shifted preferentially. Oxygen insertion seems to take place more selectively on the Mo tetrahedron sites where Bi ions are present. A comparative study and discussions on the preferential exchange in these molybdates and reoxidation sites have been reported here.

INTRODUCTION

It has been established that in the redox mechanism on Mo mixed oxide catalysts such as Bi–Mo oxides, the reduction of oxides with olefins and reoxidation with gaseous oxygen takes place in different regions (1). In such processes, the catalyst oxygen is exchanged with ^{18}O by using $^{18}O_2$ as a reactant. Studies of the Raman or IR spectra shift of γ-Bi_2MoO_6 (2, 3, 11), β-$Bi_2Mo_2O_9$ (2), α-$Bi_2Mo_3O_{12}$ (2, 11), MoO_3 (4, 12), α-$MnMoO_4$ (4, 5), $CoMoO_4$ (5), and $PbMoO_4$ (6) in which oxygen was exchanged with the ^{18}O tracer have been reported in the past. The lattice oxygen diffusion during the catalytic oxidation processes has been studied using another ^{18}O tracer method (7). We have investigated the oxidation reactions over mixed oxide catalysts (8–10). In previous literature, we have reported on the characteristic Raman band shifts of Bi–Mo oxide (11) and MoO_3 (12) catalysts exchanged with the ^{18}O tracer at the reoxidation sites in more detail.

The α-$Bi_2Mo_3O_{12}$, which is an important component in commercial catalysts, has a scheelite structure and has three kinds of Mo tetrahedra in the crystal (13, 14). With α-$MnMoO_4$, the crystal structure was determined by Abrahams *et al.* (15). The β-$CoMoO_4$ is isotypic with α-$MnMoO_4$ (16). These molybdates also have scheelite-type structures, while α-$MnMoO_4$ and β-$CoMoO_4$ have two kinds of Mo tetrahedra (15). The normal modes of Raman and IR spectra of Mo tetrahedra in α-$MnMoO_4$ crystal were determined by Kanesaka *et al.* (17) under the basis of normal coordination analysis. Hardcastle *et al.* (18, 19) have reported the direct relationship between the metal–oxygen Raman stretching frequencies and the bond strength (length) using diatomic approximation.

In the present work, we have attempted the replacement of lattice oxygen with the ^{18}O tracer using the following method:

$$\text{(Molybdate)} \xrightarrow[\text{reduc. by 1-}C_4H_8]{} \text{(molybdate)}_{\text{red.}} \xrightarrow[\text{reoxid. by } ^{18}O_2]{} \text{(molybdate)}*.$$

The (molybdate)*, such as α-$MnMoO_4$, β-$CoMoO_4$, and α-$Bi_2Mo_3O_{12}$ partly exchanged with ^{18}O tracer, were prepared. The laser Raman spectra of these exchanged oxides were obtained and compared with unexchanged oxides. The characteristic features of band shifts of three molybdate catalysts were compared and discussed, applying the correlation between the Raman band position and the Mo–O species in normal mode analysis as well as with diatomic approximation. The preferential exchange of oxygen in these molybdates and the reoxidation sites are also discussed.

METHODS

Catalysts

The α-$MnMoO_4$ supported on SiO_2 (15 at.%) was prepared as follows: the desired amounts of $Mn(NO_3)_2 \cdot 6H_2O$, ammonium heptamolybdate, and SiO_2 were mixed in the solution. After evaporation on a water bath, it was heated

[1] To whom correspondence should be addressed.

0021-9517/96 $18.00

at 723 K for 6 h. The unsupported β-$CoMoO_4$ catalyst was prepared from $Co(NO_3)_2 \cdot 6H_2O$ and ammonium heptamolybdate by heating at 773–873 K. The β-$CoMoO_4$ supported on SiO_2 (15 at.%) was prepared in the same way as the $MnMoO_4/SiO_2$ catalyst. The preparation method for α-$Bi_2Mo_3O_{12}$ supported on ZrO_2 was reported in a previous paper (11).

Procedures

The exchange of the lattice oxygen of the catalysts with ^{18}O were performed as follows: The catalysts were reduced by but-1-ene in a circulation system (ca. 290 cm^3) at ca. 4 kPa and at 773–823 K for 15–30 min. After the collection of reaction products and evacuation, reoxidation was carried out at the same temperature range and at ca. 1–3 kPa using $^{18}O_2$. The amount of ^{18}O exchanged was determined from the obtained products, i.e., the amount of buta-1,3-diene produced or from the amount of $^{18}O_2$ consumed. In the reductions the selectivities to buta-1,3-diene were 90–95% over these molybdates.

The structure of the catalysts were determined by an X-ray diffraction method using Cu K_α radiation and a Rigaku Denki Rad-rA diffractometer. The particle sizes of the molybdates were determined by a line broadening method using well-crystallized quartz as reference. The catalyst samples exchanged with ^{18}O were recorded on a JASCO NR-1000 laser Raman spectrometer. With β-$CoMoO_4$, the catalyst powders were carefully put on adhesive tape on a metal holder without pressure and grinding. An Ar–ion laser was tuned to 514.5 nm for excitation. The laser power was set at 150–200 mw. The powder samples did not reach high temperatures during the measurements. The Raman spectra data were stored on a computer and peak-shape analysis was then carried out.

RESULTS AND DISCUSSION

Characterization of the Catalysts

The $MnMoO_4/SiO_2$, $CoMoO_4$, $CoMoO_4/SiO_2$ and $Bi_2Mo_3O_{12}/ZrO_2$ structures were determined by an X-ray diffraction method. The fraction of these crystallites was determined by a comparison of the X-ray peak intensities of the catalysts and the mechanical mixtures. The crystal sizes were determined using a line broadening method and the results are shown in Table 1. The $MnMoO_4/SiO_2$ (15 at.%) catalyst contained ca. 85% crystalline α-$MnMoO_4$. The $CoMoO_4/SiO_2$ catalyst has ca. 100% of crystalline β-$CoMoO_4$. As has been reported previously (11), the crystalline percentage of α-$Bi_2Mo_3O_{12}/ZrO_2$ is ca. 40%, which is somewhat smaller than others.

$CoMoO_4$ has two crystal phases (20, 21) which are attributed to the monoclonic phase. One is stable at high temperatures (above 678 K) and the other is stable at low temperatures (below 678 K) (22). However, the former (JCPDS 21-868) (20) exists in a metastable state at room temperature. By grinding or by applying pressure, it can easily be transferred to a low temperature phase (JCPDS 25-1434) (21). In this work, the high temperature phase is designated as the β-phase and the low temperature phase as the α-phase. It should be noted that "α" is generally used for phases which are stable under normal (STP) conditions (16). In the present work, we investigated the β-$CoMoO_4$ catalyst, not α-$CoMoO_4$.

TABLE 1

Properties of the Catalysts

Catalysts	Phase	Average particle size (Å)	Amount of crystalline material (%)
Mn–Mo (1/1)/SiO_2[a] (15 at.%)	α-$MnMoO_4$	1600	85
Co–Mo (1/1)/SiO_2[a] (15 at.%)	β-$CoMoO_4$	1200	100[b]
Bi–Mo (2/3)/ZrO_2[a] (15 at.%)	α-$Bi_2Mo_3O_{12}$	1600	44
Unsupported	β-$CoMoO_4$[c]	>2000	ca. 100[b]

[a] Surface area is ca. 50 m^2g^{-1}.
[b] X-ray measurements were carried out carefully without grinding and pressure on the samples.
[c] Surface area is ca. 12 m^2g^{-1}.

The Raman spectra of β-$CoMoO_4$ and α-$MnMoO_4$ are shown in Figs. 2a and 4a. The spectra of β-$CoMoO_4$ were obtained carefully without pressure and grinding at room temperature and the results were the same as the *in situ* spectra of β-$CoMoO_4$ at high temperature reported by Kanesaka *et al.* (17). As shown in Figs. 2a and 4a, the spectra of β-$CoMoO_4$ resemble closely those of α-$MnMoO_4$. The crystal structure of β-$CoMoO_4$ is isotypic with that of α-$MnMoO_4$ (15, 16). As shown in Fig. 5a with α-$Bi_2Mo_3O_{12}$, three bands were obtained in the 900 and 800 cm^{-1} regions, respectively.

The catalysts were reduced by but-1-ene and reoxidized by $^{18}O_2$ at around 673–823 K as will be described later in this work. These procedures were repeated 5–10 times for the β-$CoMoO_4/SiO_2$ and α-$Bi_4Mo_3O_{12}/ZrO_2$ catalysts. The X-ray diffractions of the reoxidized catalysts were then measured. The diffraction patterns and linewidths were found to be nearly the same as those before treatment. Thus, the crystal phases and sizes were not remarkably changed for the β-$CoMoO_4/SiO_2$ and α-$Bi_2Mo_3O_{12}/ZrO_2$ catalysts as well as for α-$MnMoO_4/SiO_2$ by these treatments.

Crystal Structure and Raman Spectra Assignments of α-$MnMoO_4$ and β-$CoMoO_4$

The structure of α-$MnMoO_4$ is shown in Fig. 1. It has two kinds of Mo tetrahedra and two kinds of Mn octahedra. With Mo tetrahedra, Mo(1) is nearly symmetric but Mo(2)

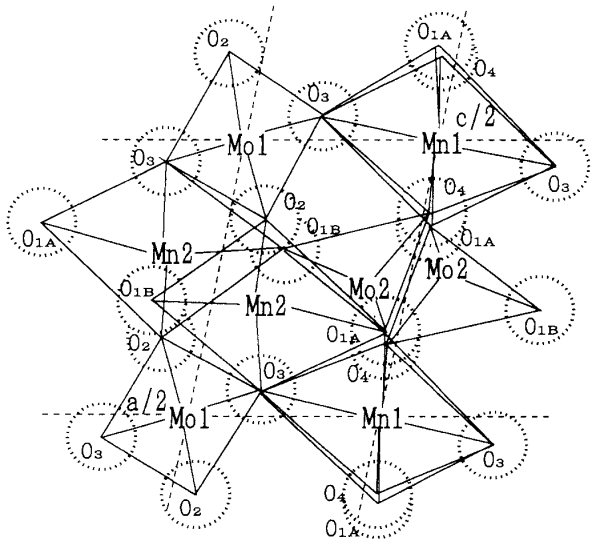

FIG. 1. Projection along the *b* axis of the structure of α-$MnMoO_4$ reported by Abrahams *et al.* (15).

is distorted and the latter is of a twin type. Table 2 shows the Mo–O distances. Kanesaka *et al.* (17) have reported the polarized Raman spectra and IR spectra of polycrystalline α-$MnMoO_4$ and have assigned the bands on the basis of a normal coordinate analysis. The stretching modes (Mo–O species) and the Raman bands assigned are also shown in Table 2 in the regions between 700 and 1000 cm^{-1}. In this work, the Raman spectrum of α-$MnMoO_4$ is as shown in Fig. 4a. There are four bands (at 825, 885, 935, and 945 cm^{-1}) present which are attributed to the stretching modes in Table 2. The bands at 850 and 735 cm^{-1} were not detected in this work. Kanesaka *et al.* (17) have reported that the bands

TABLE 2

Assigned Raman Bands of α-$MnMoO_4$ by Kanesaka *et al.* (17) and Mo–O Distances by Abrahams *et al.* (15)

Frequency mode[a]	Band[a] (cm^{-1})	Band in this work(cm^{-1})	Mo–O distance (Å)		
A_g					
Mo(2)–O(4) stretch	941	945	Mo(2)–O(4)	1.724	(2)[b]
Mo(1)–O(2) stretch	930	935	Mo(2)–O(1B)	1.738	(1)
Mo(2)–O(1B) stretch	881	885	Mo(2)–O(1A)	1.851	(1)
Mo(1)–O(3) stretch	821	825			
Mo(2)–O(1A) stretch	737	No peak	Mo(1)–O(2)	1.731	(2)
			Mo(1)–O(3)	1.795	(2)
B_g					
Mo(2)–O(4) stretch	881	(885)			
Mo(1)–O(2) stretch	850	No peak			
Mo(1)–O(3) stretch	(747)	No peak			

[a] The Raman-active stretching modes and bands by Kanesaka *et al.* (17) are shown.

[b] Numbers of bonds. Mo(1) and Mo(2) denote the Mo tetrahedra in Fig. 1. "O" denotes lattice oxygen.

TABLE 3

Assigned Raman Bands of β-$CoMoO_4$

Frequency mode[a] (cm^{-1})	Frequencies[a]	Bands in this work (cm^{-1})
A_g		
Mo(2)–O(4) stretch	946	953
Mo(1)–O(2) stretch	936	941
Mo(2)–O(1B) stretch	876	885
Mo(1)–O(3) stretch	816	825
Mo(2)–O(1A) stretch	—	No peak
B_g		
Mo(2)–O(4) stretch	(876)	(885)
Mo(1)–O(2) stretch	—	No peak
Mo(1)–O(3) stretch	—	No peak

[a] The Raman-active stretching modes and frequencies by Kanesaka *et al.* (17) which are the same as those in Table 2.

at 945 and 935 cm^{-1} both correspond to Ag modes and that the IR bands at 942 and 924 cm^{-1} should be weak in intensity from selection rules. However, these bands showed very strong IR intensities. They explained that the spectral feature should depend on an MoO_2 (or MoO) group rather than a whole tetrahedral anion.

As reported previously (15, 16), the crystal structure of β-$CoMoO_4$ is isotypic with α-$MnMoO_4$. Thus, the crystal structure of β-$CoMoO_4$ is the same as that shown in Fig. 1, replacing Mn with Co. The correlation between the normal modes of the stretching vibration and the corresponding Mo–O species for β-$CoMoO_4$ are shown in Table 3 by assuming that the normal modes are similar to those of α-$MnMoO_4$ as reported by Kanesaka *et al.* (17). However, the true Mo–O distances are unclear at present.

Raman Band Shifts of the β-$CoMoO_4$ Catalyst Exchanged with ^{18}O by a Reduction–Oxidation Method

β-$CoMoO_4/SiO_2$ (0.03 g, 15 at.%) was reduced with but-1-ene at 743–843 K. After evacuation, it was reoxidized with $^{18}O_2$ at the same temperature for 5–10 h. The selectivity to buta-1,3-diene was above 97%. The amounts of ^{18}O replaced were ca. 12–40 (in μmol). The exchange percentage were 11 and 36%, respectively, since it contains 111 μmol of oxygen as β-$CoMoO_4$ in 0.03 g. Figure 2 shows the Raman spectra of β-$CoMoO_4$ exchanged with the ^{18}O tracer. With the sample exchanged by 19%, the band at 945 cm^{-1} decreases and a new peak at around 905 cm^{-1} appears. The band at 940 cm^{-1} remains and seems to shift slightly to lower frequencies. The band at 825 cm^{-1} shows line broadening and shifts to lower frequencies. The spectra of the sample exchanged by 36% changes more markedly. The band at 825 cm^{-1} is shifted to ca. 800 cm^{-1} and its band width returns to that before the exchange. This suggests that the shift of the 825 cm^{-1} band is limited to around 800 cm^{-1}.

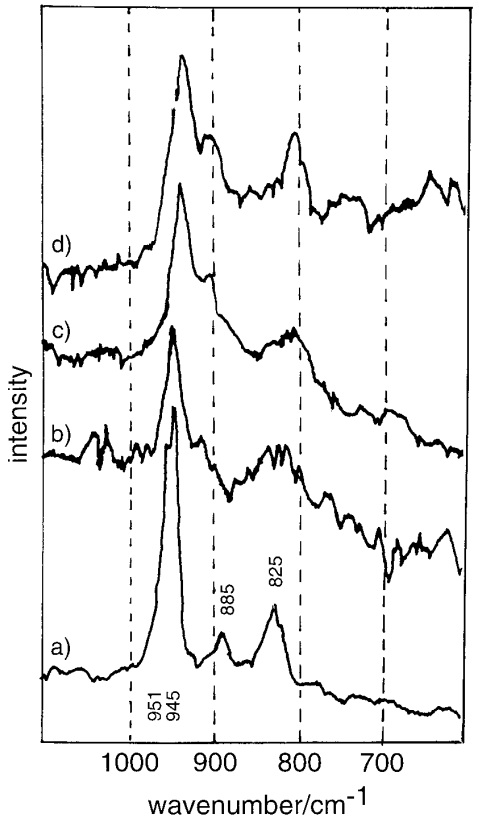

FIG. 2. Laser Raman spectra of β-$CoMoO_4$ exchanged with ^{18}O by reoxidation with $^{18}O_2$ after reduction by but-1-ene over β-$CoMoO_4/SiO_2$ (15 at.%) at 743–843 K. Amount of oxygen in the catalyst exchanged: (a) no exchange, (b) 12 μmol (ca. 11%), (c) 21 μmol (ca. 19%), and (d) 40 μmol (ca. 36%). The selectivities to buta-1,3-diene were above 97%.

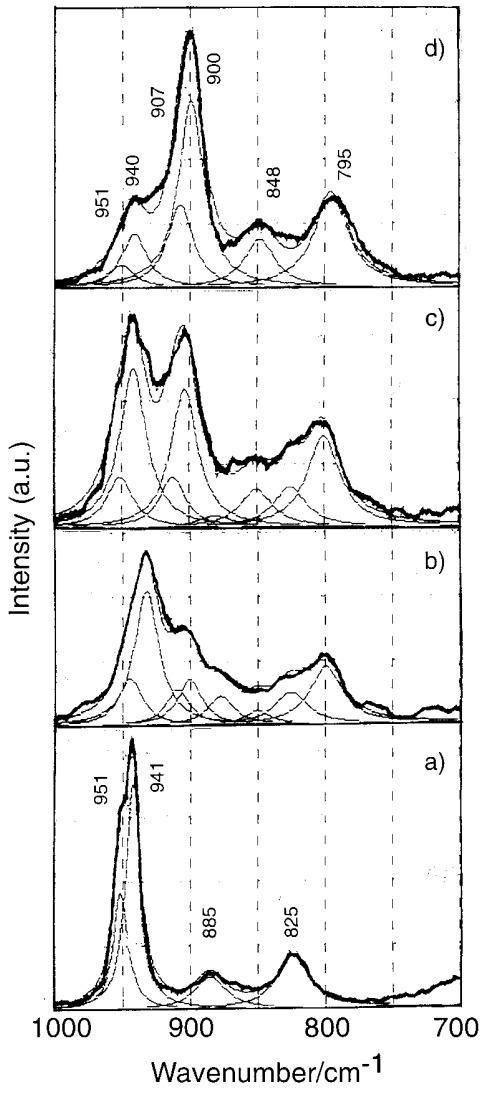

FIG. 3. Raman spectra of β-$CoMoO_4$ almost exchanged with ^{18}O and band shape analysis of some observed spectra. (a) No exchange (Fig. 2a sample), (b) Average 19% exchanged (Fig. 2c sample), (c) <36% of oxygen of unsupported β-$CoMoO_4$ was exchanged, (d) more than 90% of unsupported β-$CoMoO_4$ oxygen was exchanged with ^{18}O. Thick lines are observed spectra. Thin lines denote the separated peaks and sum of them.

In order to obtain the true band shifts of β-$CoMoO_4$ exchanged with ^{18}O, reduction by but-1-ene and reoxidation with $^{18}O_2$ were repeated as many times as possible. Figures 3c and 3d show the spectra of unsupported β-$CoMoO_4$ exchanged with ^{18}O. The curve fittings were better in the case of the Lorenzian rather than the Gaussian function. The same half widths were used for the original and shifted bands. As shown in the figures, both the original and the shifted bands show line broadening. These may be caused by the reduction–oxidation treatments. From Figs. 3a, 3c, and 3d, the bands at 951, 941, 885, and 825 cm^{-1} were observed to shift to 907, 900, 848, and 795 cm^{-1}, respectively. The shift intervals were determined as 44, 41, 37, and 30 cm^{-1}, respectively, which are nearly the same as those calculated theoretically as ca. 45 cm^{-1} at around 900 cm^{-1} and 40 cm^{-1} at around 800 cm^{-1}.

In order to understand the details of the shifts, band shape analysis was carried out with the results of Fig. 2. An example of curve fitting is shown in Fig. 3b. The better fittings were accomplished when 944, 937, 885, and 825 cm^{-1} were used for the original positions and 907, 900, 850, and 795 cm^{-1} for the shifted positions as described above. There appeared to be some decreasing of the original frequencies at 950–945 cm^{-1} as well as band broadening with increasing the concentration of ^{18}O. The shifted fractions calculated by the peak area are shown in Table 4. The results indicate that all oxygen ions of Mo(1) and twin Mo(2) tetrahedra are exchanged with an increase in ^{18}O. The results suggest that the oxygen of Mo(1)–O(3), which corresponds to 825 cm^{-1}, and Mo(2)–O(4) which corresponds to 950 cm^{-1}, are exchanged preferentially. Table 4 shows large differences appearing between the average exchange percentage and the fraction of the shifted band. This suggests that Raman information comes from near the surface of β-$CoMoO_4$ and that the exchanged oxygen ions are localized near the surface of

TABLE 4

Fraction of Raman Band Intensity of β-$CoMoO_4$ Exchanged with ^{18}O

Average percentage of exchanged ^{18}O	Oxygen species and fractions shifted			
	Mo(2)–O(4) $(I_{908}/(I_{951}+I_{908}))$	Mo(1)–O(2) $(I_{900}/(I_{937}+I_{900}))$	Mo(2)–O(1) $(I_{850}/(I_{885}+I_{850}))$	Mo(1)–O(3) $(I_{800}/(I_{825}+I_{800}))$
11	0.1	0.08	—	0.2
19	0.4	0.25	0.3	0.6
27[a]	0.4	0.1	0.3	0.7
<36[a]	0.5	0.5	0.75	0.7
36	0.4	0.25	0.7	0.8

Note. I denotes intensity in terms of Raman peak area separated as shown in Fig. 3. Numerals in subscript are band positions. The β-$CoMoO_4/SiO_2$ (15 at.%) catalyst was used.

[a] Unsupported β-$CoMoO_4$ catalyst.

the β-$CoMoO_4$ catalyst. These features are found with the supported and unsupported β-$CoMoO_4$ (Table 4).

Raman Band Shifts of the α-$MnMoO_4$ Catalyst Exchanged with ^{18}O by a Reduction–Oxidation Method

α-$MnMoO_4/SiO_2$ (0.03 g, 15 at.%) was reduced with but-1-ene at 773 K. After evacuation, the sample was reoxidized with $^{18}O_2$ at 773 K. The exchange percentages were calculated as 17 and 26% since the total amount of α-$MnMoO_4$ oxygen in the catalyst was ca.130 μmol. Figure 4a shows the spectrum of the catalyst after reoxidation by ordinary $^{16}O_2$. With the sample exchanged with ^{18}O by ca. 17% (Fig. 4b), the band at 945 cm^{-1} decreases and the band at around 900 cm^{-1} is increasing slightly. The bands at 935, 885, and 825 cm^{-1} retain their positions though the peaks show some line broadening. The spectrum for the 26% sample (Fig. 4c) shows a shape similar to that of (Fig. 4b) and new shoulders appear at around 850 and 800 cm^{-1}. Ozkan *et al.* (4) have reported the ^{18}O exchange studies with the $MnMoO_4/MoO_3$ system and that the α-$MnMoO_4$ had less activity in replacement with ^{18}O. However, a slight increase in intensity was observed at around 900 cm^{-1}.

In order to investigate the shift change in detail, peak shape analysis was carried out with these spectra (Fig. 4). The shift intervals for α-$MnMoO_4$ after exchange were the same as those for β-$CoMoO_4$ due to its isotypic structure with β-$CoMoO_4$ as well as similar Raman spectra to β-$CoMoO_4$. The bands at 945, 935, 885, and 825 cm^{-1} shift to 900, 895, 850, and 795 cm^{-1}. Curve fittings were carried out using these peaks and the Lorenzian function described with the β-$CoMoO_4$ catalyst. The exchange fraction was compared for each band between the original peak area and the shifted one and they are shown in Table 5. With the average 17% sample, the fraction is ca. 0.10 for the 945 cm^{-1} band and 0.02 for the 935 cm^{-1} band. With the average 26% sample, the 945 cm^{-1} band shifts with the fraction ca. 0.3 and those of the other bands are 0.1–0.2. According to Table 2, the 945 cm^{-1} band corresponds to the Mo(2)–O(4) in the Mo(2) tetrahedron. Reoxidation from gaseous oxygen takes place preferentially on the sites corresponding to the former, i.e., the 945 cm^{-1} band. According to Matsuura *et al.* (5), the band at 875 cm^{-1} (885 in this work) shifted among four bands using C_3H_6 and $^{18}O_2$. However, the disparity from our work is unclear at present.

Raman Band Shifts of the α-$Bi_2Mo_3O_{12}$ Exchanged with ^{18}O by a Reduction–Oxidation Method

In order to obtain the final positions of the shifted bands of α-$Bi_2Mo_3O_{12}$ after sufficient exchange with ^{18}O, reduction by but-1-ene and reoxidation by $^{18}O_2$ were repeated

TABLE 5

Fraction of Raman Band Intensity of α-$MnMoO_4$ Exchanged by ^{18}O

Average percentage of exchanged ^{18}O	Oxygen species and fraction shifted			
	Mo(2)–O(4) $(I_{905}/(I_{945}+I_{905}))$	Mo(1)–O(2) $(I_{895}/(I_{935}+I_{895}))$	Mo(2)–O(1) $(I_{850}/(I_{885}+I_{850}))$	Mo(1)–O(3) $(I_{795}/(I_{825}+I_{795}))$
17	0.11	0.02	0	0
26	0.3	0.1	0.2	0.1

Note. I denotes intensity in terms of Raman peak area separated as shown in Fig. 4. Numerals in subscript are band positions.

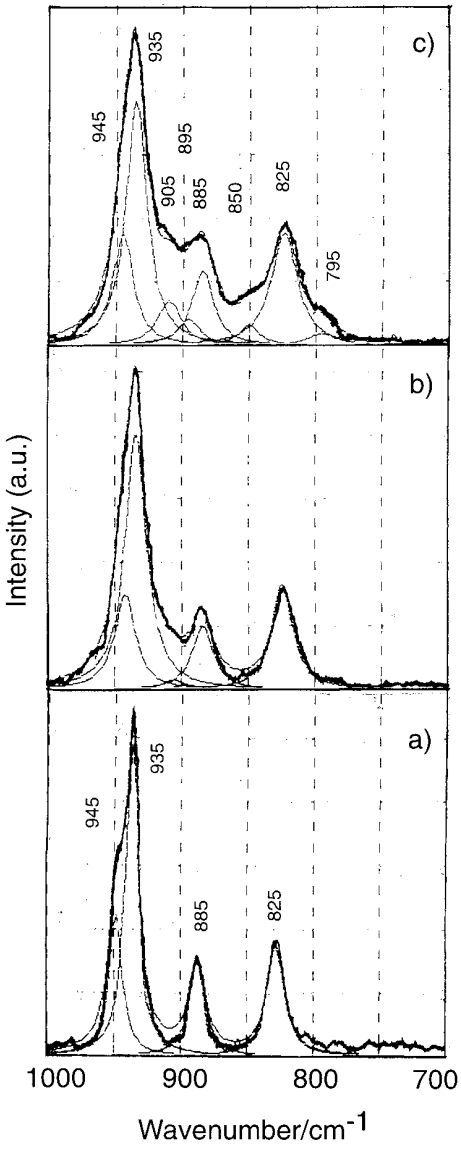

FIG. 4. Laser Raman spectra of α-$MnMoO_4$ exchanged with ^{18}O by reoxidation with $^{18}O_2$ after reduction by but-1-ene over α-$MnMoO_4/SiO_2$ (15 at.%) at 773 K. We used 0.03 g of catalyst. Amount of oxygen in the catalyst exchanged: (a) no exchange, (b) 22 μmol (ca. 17%), (c) 34 μmol (ca. 26%). The selectivities to 1,3-butadiene were ca. 90%. Thick lines are observed spectra. Thin lines are separated peaks and sum of them.

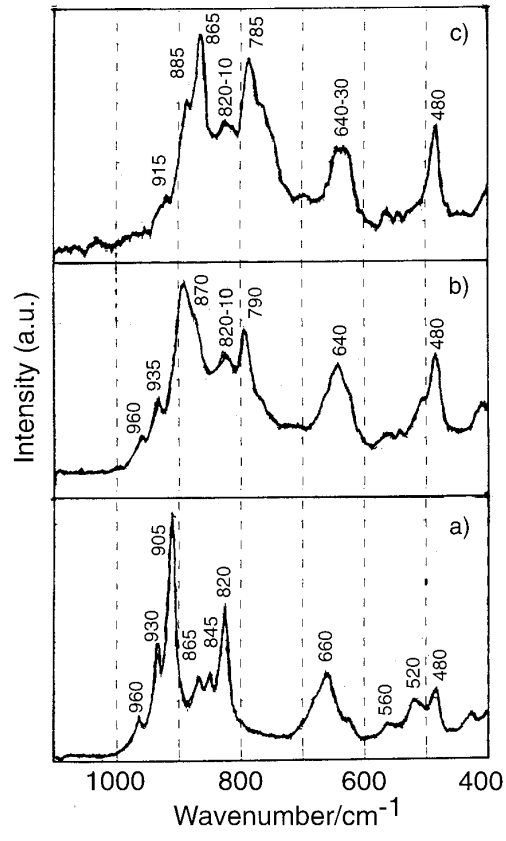

FIG. 5. Laser Raman spectra of α-$Bi_2Mo_3O_{12}$ deeply exchanged with ^{18}O. (a) No exchange sample. (b) The reduction by but-1-ene and reoxidation by $^{18}O_2$ were repeated five times at 700 K (one time: ca. 25–30 μmol of ^{18}O was replaced in 0.05 g of the catalyst. (c) Repeated 10 times; all oxygen ions seem to be replaced with ^{18}O. The selectivities to buta-1,3-diene were ca. 90%. The spectra in the range from 400 to 630 cm^{-1} contain those of ZrO_2.

many times over this catalyst. Before exchange, the α-$Bi_2Mo_3O_{12}$ catalyst has six bands at 1000–800 cm^{-1} as shown in Fig. 5a. At the high degree of ^{18}O exchange (Fig. 5b), the bands at 860, 845, and 820 cm^{-1} almost shift and the band at 660 cm^{-1} also shifts to 640 cm^{-1}. The bands in the 900 cm^{-1} region remains unshifted. Finally, Fig. 5c suggests that the bands at 960, 930, 905, 865, 845, and 820 cm^{-1} shift to 915, 885, 870, 820–805, and 785 cm^{-1}. The theoretical shifts in the 900–800 cm^{-1} region were calculated as 45–40 cm^{-1} which are nearly equal to the shift values of 45–35 cm^{-1} observed above.

The results of the Raman spectra of α-$Bi_2Mo_3O_{12}$ exchanged with a small amount of the ^{18}O tracer are shown in the Fig. 6. Two bands at 860 and 845 cm^{-1} decrease markedly. Those at 960, 930, and 905 cm^{-1} scarcely change and new bands at 780–800 cm^{-1} appear. These features are in sharp contrast to those of α-$MnMoO_4$ and β-$CoMoO_4$. The peak shape analysis was carried out between 1000 and 800 cm^{-1} using the shift band results. As can be seen with the sample which has an average exchange of 10% (Fig. 6), three peaks at around 865–820 cm^{-1} are separated. Table 6 shows that the fractions of shifted bands are bigger for 865 and 845 cm^{-1} bands than those for the 820 cm^{-1} band. The high fraction values ($\sim$0.6) compared to the average exchange percentage ($\sim$10%) indicates that the exchange occurs at the surface of catalysts and oxygen insertion takes place more selectively. With the bands at 960–905 cm^{-1}, a ratio of $I_{960} : I_{930} : I_{905}$ was obtained by shape analysis as 0.11 : 0.37 : 1.0 for the spectra shown in Fig. 5a while the 10% sample shown in Fig. 6a is calculated as 0.10 : 0.34 : 1.0 which is nearly the same. With the 20% sample, the band

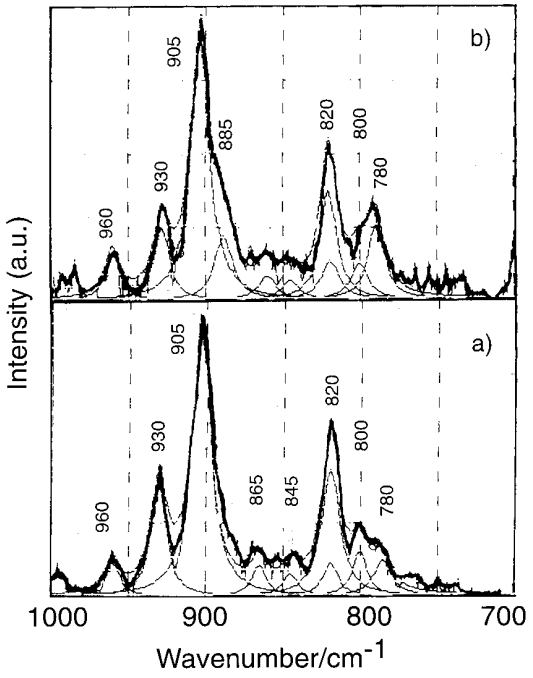

FIG. 6. Laser Raman Spectra of α-$Bi_2Mo_3O_{12}$ exchanged with ^{18}O by reoxidation with $^{18}O_2$ after reduction by but-1-ene at 673 K in a low exchange region. We used 0.03 g of catalyst. Amount of oxygen in the catalyst exchanged: (a) 8 μmol (ca. 10%), (b) 17 μmol (ca. 20%). Band shape analysis was carried out with (a) and (b) spectra. Thick lines denote observed spectra and thin lines denote separated bands.

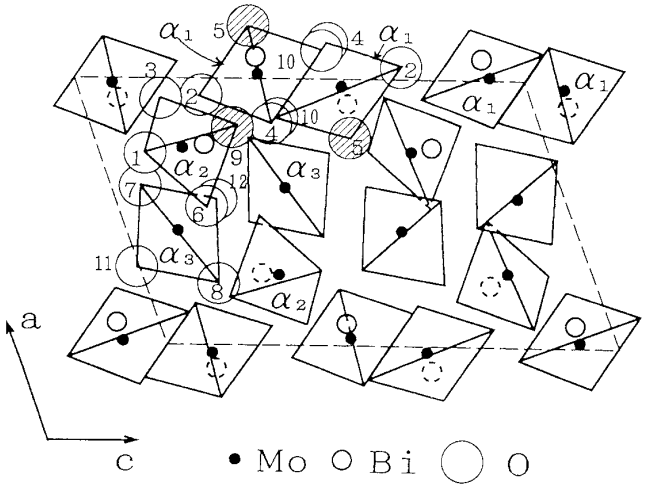

FIG. 7. Projection along the *b* axis of the structure of α-$Bi_2Mo_3O_{12}$ reported by Cesari *et al.* (13) and Elzen *et al.* (14). α_1, α_2, and α_3 denote the Mo tetrahedra. The numerals denote the oxygen position numbers reported by Elzen *et al.* (14). The shaded oxygen circles denote the well-exchanged positions (see text).

at around 890 cm^{-1} which shifted from 930 cm^{-1} becomes bigger. On the other hand, the band at ca. 870 cm^{-1} which shifted from 905 cm^{-1} does not become bigger (Fig. 6b). The shape analysis of the 660 cm^{-1} band was difficult since it is an overlap of several peaks before exchange (22).

Crystal Structure and Raman Band Assignment for α-$Bi_2Mo_3O_{12}$

Figure 7 shows the structure of α-$Bi_2Mo_3O_{12}$ reported by Cesari *et al.* (13). As can be seen, it consists of two kinds of twin tetrahedra, i.e., $\alpha_1\,\alpha_1$ and $\alpha_2\,\alpha_3$. The $\alpha_1\,\alpha_1$ twin tetrahedron has a symmetry center. α_1 and α_2 have Bi ions adjacent to the tetrahedra, while there is a Bi ion vacancy near the α_3 tetrahedron. Elzen *et al.* (14) have also reported the structure and Mo–O distances of each tetrahedron. Assignments of Raman Spectra of α-$Bi_2Mo_3O_{12}$ in accordance with normal mode analysis have not yet been reported. Matsuura *et al.* (23) reported that the bands at around 900 and 800 cm^{-1} can be attributed to the stretching modes of each tetrahedral species applied to the Cotton–Wing relation (24), i.e., 960 (α_3), 930 (α_1), 905 (α_2), 860 (α_1), 845 (α_2), and 820 (α_3). Using the correlation between Raman bands and Mo–O distances for the α-phase by the diatomic approximation as proposed by Harcastle and Wachs (18, 19), the bands, the corresponding Mo–O, and tetrahedron species (Fig. 7) are as follows: 960 cm^{-1} (1.68 Å, Mo(3)–O(12)), 930(1.69 Å, Mo(1)–O(4)), 905(1.72 Å, Mo(2)–O(1)), 860(1.72 Å, Mo(1)–O(5)), 845(1.73 Å, Mo(2)–0(9)), and 820(1.78 Å, Mo(3)–O(11)). In these assignments, we added some modifications (11) and these results are the same as those by Matsuura *et al.* (23). The broad band at around 650 cm^{-1} may correspond to several band overlappings and to the 1.85- to 1.90 Å Mo–O oxygen of the α_{1-3} tetrahedra.

TABLE 6

Fraction of Raman Band Intensity of α-$Bi_2Mo_3O_{12}$ Exchanged with ^{18}O

Average percentage of exchanged ^{18}O	Fraction of the shifted band		
	Mo(1)–O(5) $(I_{820}/(I_{860}+I_{820}))$	Mo(2)–O(9) $(I_{800}/(I_{845}+I_{800}))$	Mo(3)–O(11) $(I_{785}/(I_{820}+I_{785}))$
10	0.5	0.65	0.2
20	0.6	0.6	0.4

Note. I denotes in terms of Raman band area separated as shown in Figs. 6a and 6b. In the shape analysis of 860–785 peaks, the ratio of I_{860}: I_{845}: I_{820} (1 : 1 : 3) in the original spectra (Fig. 5a) was used as a basis.

Reoxidation Sites of α-$Bi_2Mo_3O_{12}$

In the reoxidation step, the oxygen seems mainly to be inserted at the sites giving rise to the 860 and 845 cm^{-1} bands, i.e., oxygen at 1.72 and 1.73 Å in the α_1 and α_2 tetrahedra, respectively. Two Mo tetrahedra of $\alpha_1\alpha_1$ are situated in the adjacent Bi ions (Fig. 7), while the $\alpha_2\alpha_3$ tetrahedra includes a Bi ion vacancy for α_3 and the presence of Bi ion for α_2. The band at 820 cm^{-1} which corresponds to the tetrahedron

TABLE 7

Comparison of Exchange Fractions of Each Lattice Oxygen Species of the Catalysts at a Low Average Exchange

Catalyst	Average percentage exchanged of ^{18}O	Exchange fractions of oxygen species					
		Mo(3)=O	Mo(2)=O	Mo(1)=O	Mo(3)–O	Mo(2)–O	Mo(1)–O
α-$Bi_2Mo_3O_{12}$	10	0	0	0	0.2	0.65	0.5
β-$CoMoO_4$	11		0.1	0.08		0	0.2
α-$MnMoO_4$	17		0.1	0.02		0	0

Note. Mo(3, 2, 1) corresponds to α_3, α_2, and α_1 of α-$Bi_2Mo_3O_{12}$ and to Mo2 and Mo1 of β-$CoMoO_4$ and α-$MnMoO_4$, respectively. Mo=O denotes the shortest bond (double bond character) in the Mo tetrahedra of each catalyst. Mo–O denotes long bonds next to the shortest bond.

α_3 shifted less than that at 845 cm^{-1}, to α_2 at low ^{18}O exchange. This tendency is the same as that of α-$Bi_2Mo_3O_{12}$ after the oxidation reaction using the $C_3H_6 + {}^{18}O_2$ mixture (11). The terminal Mo–O(930 cm^{-1}) of α_1 was exchanged but that (905 cm^{-1}) of α_2 was not exchanged even at high ^{18}O concentrations. These results also suggest a more selective insertion of oxygen at α_1 tetrahedra. In Fig. 7, the positions of oxygen which are well exchanged are also shown. The positions of oxygen insertion are attributed to Mo(1)–O(5) in α_1 and Mo(2)–O(9) in α_2. The positions which are not exchanged are the Mo(1)–O(4) and Mo(2)–O(1) which are the shortest in the tetrahedra (14). The O(5) oxygen also coordinates to the Bi(1) ion with a distance of 2.94 Å. The O(9) oxygen coordinate to the Bi(2) ion with a distance of 2.61 Å. These two oxygen ions are very far from each Bi ion among the eight coordinated oxygen (14). It is generally accepted that the reaction of the oxides with alkenes and reoxidation by gaseous oxygen occur in different regions (1). Thus, If the reoxidation takes place on the O(5) and O(9) positions in Fig. 7, the oxygen reacted with but-1-ene may be another position in the α_1 and α_2 Mo tetrahedra. Other lattice oxygens corresponding to the bands in the range 700–600 cm^{-1}, i.e., weaker Mo–O oxygen, will participate in oxidation reactions. A quantitative discussion, however, would be difficult at present.

Burlamacchi *et al.* (25) and Peacock *et al.* (26) have studied the reduction of α-$Bi_2Mo_3O_{12}$ using ESR spectroscopy. Both groups reported the observation of Mo^{5+} formation in the reduced α-phase. Other studies of reoxidation on Bi–Mo oxide catalysts after reduction have been reported (27–29). Bradzil *et al.* (29) have explained that the activation energy of reoxidation at surface vacancies is very different from that at bulk vacancies. They also discussed the restructuring between a corner-linked structure and edge-linked one in the case of Mo polyhedra. Snyder and Hill have discussed Mo^{5+} formation and the restructuring of Mo polyhedra (1). The preferential exchange of these Mo–O species may occur via such a restructuring mechanism since α-$Bi_2Mo_3O_{12}$ consists of twin Mo tetrahedral structures.

SUMMARY

(1) Table 7 shows a comparison of results among molybdate catalysts. With α-$MnMoO_4$, the bands at 945 cm^{-1} corresponding to the shortest Mo=O of the Mo(2) tetrahedron shifted preferentially to lower frequencies at a low degree of exchange. Oxygen insertion seems to take place initially at this vacancy. Most oxygens of two kinds of Mo tetrahedra were replaced with increase in the degree of exchange. With β-$CoMoO_4$ a slight preferential shift of the 950 and 825 cm^{-1} bands were observed. However, at a high degree of exchange, all oxygen ions were replaced with ^{18}O as with α-$MnMoO_4$. These results indicate that the random migration of anion vacancies tend to occur on these catalysts.

(2) α-$Bi_2Mo_3O_{12}$ has two kinds of twin Mo tetrahedra and three Mo tetrahedra. The bands at 865 and 845 cm^{-1} were shifted preferentially, while the bands at 960–905 cm^{-1} which correspond to the terminal Mo=O bonds did not initially exchange greatly as shown in the Table 7 and Fig. 7. Such a selective exchange and oxygen uptake seems to be originated from twin Mo tetrahedra structure and from the presence of Bi ions near the Mo tetrahedra.

(3) The activity order for reduction by but-1-ene was obtained as follows: α-$Bi_2Mo_3O_{12} > \beta$-$CoMoO_4 \gg \alpha$-$MnMoO_4$. The twin Mo tetrahedra with the presence of Bi ions seem to be an important structure for the selective reoxidation step as well as for hydrogen abstraction. Very low activity of α-$MnMoO_4$ may be originated from the low activity of the shortest Mo=O in Mo tetrahedra.

ACKNOWLEDGMENTS

We extend our special thanks to Prof. I. Kanesaka of Toyama University for his helpful discussion and instructions. Also we thank Dr. H. Miyata for his help with the computer band-shape analysis. We are grateful to Mr. H. Numata for his part in carrying out the experiments.

REFERENCES

1. Snyder, T. D., and Hill, G. C., Jr., *Catal. Rev. Sci. Eng.* **31**, 43 (1989); Grasselli, R. K., and Burrington, J. D., *Adv. Catal.* **30**, 133 (1981).

2. Hoefs, E. V., Monnier, J. R., and Keulks, G. W., *J. Catal.* **57**, 331 (1979).
3. Grasselli, R. K., *Appl. Catal.* **15**, 127 (1985); Glaeser, L. C., Brazdil, J. F., Hazle, M. A., Mehicic, M., and Grasselli, R. K., *J. Chem. Soc., Faraday Trans. I*, **81**, 2903 (1985).
4. Ozkan, U. S., Smith, M. R., and Driscoll, S. A., *J. Catal.* **134**, 24 (1992).
5. Matsuura, I., Hashiba, H., and Kanesaka, I., *Chem. Lett.* 533 (1986).
6. Kanesaka, I., Kirishiki, M., and Matsuura, I., *J. Raman, Spectrosc.* **23**, 201 (1992).
7. Ueda, W., Morooka, Y., and Ikawa, T., *J. Chem. Soc., Faraday Trans. I* **78**, 495 (1982); Matsuura, I., and Kirishiki, M., *Chem. Lett.* 1441 (1986); Coulson, D. R., Mills, P. L., Kourtakis, K., Wijnen, P. W., Lerou, J. J., and Manzer, L. E., *in* "Proceedings, 10th International Congress on Catalysis, Budapest, 1992" (L. Guczi, F. Solymosi, and P. Tetenyi, Eds.). Akadémiai Kiads, Budapest, 1993.
8. Ono, T., Nakajyo, T., and Hironaka, T., *J. Chem. Soc., Faraday Trans.* **86**, 4077 (1990).
9. Ono, T., Kiryu, M., Komiyama, M., and Kuczkowski, R. L., *J. Catal.* **127**, 698 (1991).
10. Ono, T., Yamanaka, T., Kubokawa, Y., and Komiyama, M., *J. Catal.* **109**, 423 (1988).
11. Ono, T., and Ogata, N., *J. Chem. Soc., Faraday Trans.* **90**, 2113 (1994).
12. Ono, T., Numata, H., and Ogata, N., *J. Mol. Catal.* **105**, 31 (1996).
13. Cesari, M., Perego, G., Zazzetta, A., Manara, G., and Notari, B., *Inorg. Nucl. Chem.* **33**, 3595 (1971).
14. Elzen, A. F. V., and Rieck, G. D., *Acta Crystallogr.* Sect.B, **29**, 2433 (1973).
15. Abrahams, S. C., and Reddy, J. M., *J. Chem. Phys.* **43**, 2533 (1965).
16. Sleight, A. W. and Chamberland, B. L., *Inorg. Chem.* **7**, 1672 (1968).
17. Kanesaka, I., Hashiba, H., and Matsuura, I., *J. Raman Spectrosc.* **19**, 213 (1988).
18. Hardcastle, F. D., and Wachs, I. E., *J. Raman Spectrosc.* **21**, 683 (1990).
19. Hardcastle, F. D., and Wachs, I. E., *J. Phys. Chem.* **95**, 10763 (1991).
20. Courtine, P., Cord, P. P., Pannetier, G., Daumas, J. C., and Montarnal, R., *Bull. Soc. Chim. France* 4816 (1968).
21. Smith, G. W., and Ibers, J. A., *Acta. Crystallogr.* **19**, 269 (1965).
22. Get'man, E. I., and Marchenko, V. I., Russ. J. *Inorg. Chem.* **25**, 1072 (1980).
23. Matsuura, I., Shut, R., and Hirakawa, K., *J. Catal.* **63**, 152 (1980).
24. Cotton, F. A., and Wing, R. M., *Inorg. Chem.* **4**, 867 (1965).
25. Burlamacci, L., Martini, G., and Ferroni, E., *J. Chem. Soc. Faraday Trans. I* **68**, 1586 (1972).
26. Peacock, J. M., Sharp, M. J., Parker, A. J., Ashmore, P. G., and Hockey, J. A., *J. Catal.* **15**, 379 (1969).
27. Matsuura, I., and Schuit, G. C. A., *J. Catal.* **20**, 19 (1971).
28. Uda, T., Lin, T., and Keulks, G. W., *J. Catal.* **62**, 26 (1980).
29. Brazdil, J. F., Suresh, D. D., and Grasselli, R. K., *J. Catal.* **66**, 347 (1980).